(A)

(B)

(C)

(D)

(E)

Fig. 2.   Evaluation of Tumor Vascular Permeability Using DCE-MRI
    Protocol of the experiment (A), mean Gd uptake curves in mice bearing colon 26 tumors before and after intraperitoneal A–83–01 injection using Gd-DTPA (B) and Gd-L (C) as a contrast agent, and the initial area under the Gd concentration-time curve over 60 s (IAUGC$_{60}$) with Gd-DTPA (D) and Gd-L (E). (A) Single-treated mice were intraperitoneally injected with A–83–01 at 0 h, and repeat-treated mice were injected at 0 h and 21 h. Values in (C) and (D) represent the mean±S.D. (n=3–6).

曲線から 60 秒間の AUC（IAUGC$_{60}$）を算出した
［Fig. 2 (D) and (E)］．A–83–01 の繰り返し投与に
よって，IAUGC$_{60}$ は Gd-DTPA では約 1.8 倍，Gd-L
では 3.8 倍に上昇した．A–83–01 の繰り返し投与は
腫瘍血管の透過性を高め，特に Gd-L のような微粒
子の移行性を高めることが明らかになった．

　これらの腫瘍内造影剤濃度推移を 2-コンパート
メントモデルで解析し，v$_\mathrm{p}$ と K$^\mathrm{trans}$ を算出した
（Fig. 3）．A–83–01 単回投与 3 時間後においては，
6 匹中 2 匹で高い v$_\mathrm{p}$ と K$^\mathrm{trans}$ を示したが，他の 4 匹
では上昇がみられず大きなばらつきを示した．A–

83–01 単回投与の 24 時間後では，v$_\mathrm{p}$ や K$^\mathrm{trans}$ は投与
前と同じ値を示し，変化しなかった．A–83–01 繰
り返し投与の 24 時間後では，Gd-DTPA を用いた
すべてのマウスで v$_\mathrm{p}$ と K$^\mathrm{trans}$ が増加しており，Gd-L
においても同様に増加した．v$_\mathrm{p}$ は造影剤の静脈内
投与直後に，腫瘍血管に流れ込んだ造影剤の量に依
存する．そのため v$_\mathrm{p}$ の増加は，血流のある腫瘍血
管体積が増加したと考えられる．また，K$^\mathrm{trans}$ は腫
瘍血管から腫瘍間質への移行性を示し，A–83–01
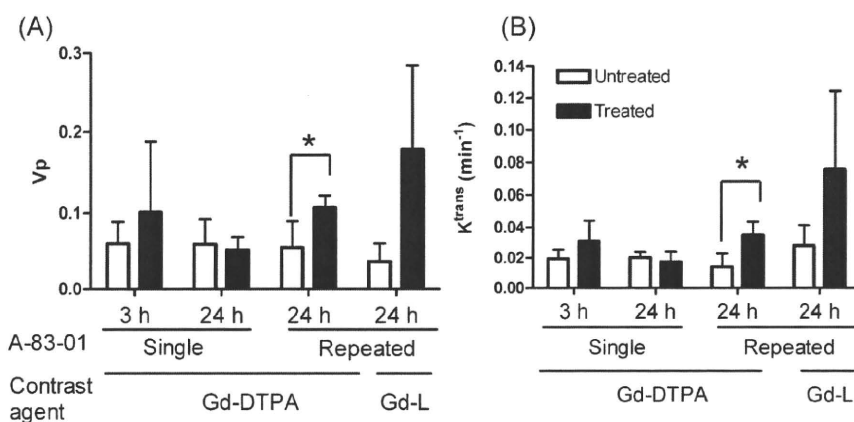により血管透過性が亢進したと考えられる．

Fig. 3. Values of Fractional Plasma Volume (v_p) (A) and Volume Transfer Constant (K^{trans}) between the Blood Plasma and the v_e (B)

Mice bearing colon 26 tumors were examined before and at 3 h and 24 h after single or repeated A–83–01 injection using Gd-DTPA and Gd-L as a contrast agent. Each value represents the mean±S.D. (n=3–6). * p<0.05.

5.　A-83-01 投与後の腫瘍の組織学的評価と水の見かけの拡散係数

腫瘍内の微小環境変化を組織学的に評価するために，A-83-01 繰り返し投与後の腫瘍切片を作製し，顕微鏡観察を行った．ヒト膵臓がん BxPC3 移植腫瘍において TGF-β 阻害薬（LY364947）を投与すると，腫瘍血管のペリサイトは減少すると報告されている．[4] colon26 細胞移植腫瘍においては，α-smooth muscle actin（SMA）に対する免疫染色によって確認されるペリサイトの分布は少なく，A-83-01 繰り返し投与によってペリサイトは逆に増加した．[13] 腫瘍によって血管の構築性が異なるために，TGF-β 阻害薬による血管への作用が異なることが推察された．

腫瘍細胞の形態は類円形ないしは紡錘型を示しており，A-83-01 繰り返し投与群と未投与群との間に形態の差はみられなかった．血管の形態は，未処置群では歪な形態の腫瘍血管が認められたが，A-83-01 繰り返し投与の 24 時間後では血管の形態が円形又は楕円形の正常に近い状態に変化しており，腫瘍における血管面積は減少する傾向が確認された〔Fig. 4(A)〕．さらに抗 Ki67 抗体を用いた免疫染色により増殖期にある細胞核を染色して Ki67 陽性細胞の割合を算出したところ，腫瘍細胞の中心部では陽性細胞が少なく，辺縁部では陽性細胞が多かった．また，腫瘍血管周辺部において増殖期にある細胞数を比較すると，A-83-01 繰り返し投与により有意に増加していた〔Fig. 4(B)〕．腫瘍新生血管で
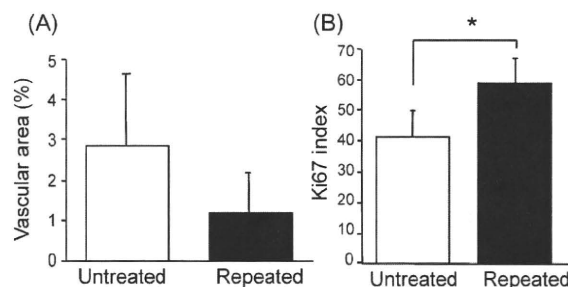

Fig. 4. Tumor Vascularity (A) and Ki67 Index (B) of Colon 26 Tumors before and after Repeated A–83–01 Injection

(A) Percentage of the vascular areas within the tumors. (B) Percentage of Ki67 positive proliferating cells in the perivascular region. Each value represents the mean±S.D. (n=5). * p<0.05.

は血流のうっ帯など機能的に障害があり，十分な酸素や栄養を届けることが困難である．増殖期にある細胞数は周辺の酸素状態と関連していると考えられ，A-83-01 処置により血流が回復し周辺環境が改善したと推測される．腫瘍摘出直前に Hoechst33342 を尾静脈から投与して血流のある血管を染色した結果，A-83-01 の処置後に Hoechst33342 の蛍光強度が増大していた（未発表データ）ことからも，A-83-01 処置による血流の回復が示唆された．

これらの変化は，Jain[14] が提唱する血管正常化（normalization）に類似した結果であると考えられる．血管正常化とは，血管新生阻害薬を用いた治療において併用した抗がん薬や放射線治療のような血流に依存する効果を高めることから，血管新生阻害薬が未熟で低効率な微小血管を取り除き，血管の構

造や機能を一時的に正常に近づけたことにより併用
治療の効果を高めるという仮説である．A-83-01
の繰り返し投与によって，血管形態においては円形
に近づきペリサイト被覆が増加したことや，DCE-
MRI の評価にて血漿体積（v_p）の増大などにより
血流の回復が示唆されたことから，一過的な血管正
常化効果が微粒子の移行性亢進に関与する可能性が
示唆された．

　さらに，MRI により拡散強調画像を取得し，見か
けの拡散係数（apparent diffusion coefficient, ADC）
を求め，A-83-01 の処置による腫瘍内の水分子の
動きの変化を評価した（Fig. 5）．ここでの ADC 値
は，腫瘍内の血流を除外し，細胞外液と細胞内液の
体積変化の指標として用いた．A-83-01 の単回投
与 3 時間と 24 時間後では，ADC 値は投与前と比
べて変化がなかったのに対し，繰り返し投与では有
意に低下していた．細胞外液の水は，細胞内液と比
較して自由度が高いので，拡散係数が大きくなる．
腫瘍組織観察から A-83-01 を投与しても細胞形態
の変化やネクローシスはみられないことから，細胞
内液の体積変化は少なく，ADC 値の低下は細胞外
液の減少を反映したと考えられる．腫瘍血管の正常
化に伴う血流の回復によって，間質圧の低下が起こ
り，薬物の移行性が高まることが報告されてい
る．[15] 回復した血流が腫瘍の過剰な細胞外液を回収
し，それによって腫瘍間質圧が低下したことが，
Gd-L の透過性亢進に寄与した可能性も考えられる．
A-83-01 による Gd-L の透過性亢進の作用メカニズ
ムについては，さらに詳細な検討が必要である．

6. A-83-01 併用によるドキソルビシン封入リポソームの抗腫瘍効果

　DCE-MRI の結果より，A-83-01 の併用は微粒子
の腫瘍移行性を高めることが示された．そこで，A
-83-01 併用時のドキソルビシン封入血中滞留性リ
ポソーム（SL）と葉酸修飾リポソーム（F-SL）の
腫瘍集積性と抗腫瘍効果の評価を行った．ここで
は，葉酸受容体を発現するマウス肺がん M109 細胞
を皮下移植したマウスを用いた．M109 腫瘍におい
ても，A-83-01 投与 3 時間後において Gd-L での
IAUGC の増加がみられ，24 時間後には未投与時と
同程度へ戻り，colon26 腫瘍と同様に一過的な作用
が認められた．[16] A-83-01 の併用により，SL 及び
F-SL の投与 24 時間後の腫瘍集積量は 1.5 から 1.7
倍増大し，[16] F-SL においては抗腫瘍効果が有意に
増大した（Fig. 6）．A-83-01 の作用が一過的であ
ることから，受動的腫瘍送達の SL と能動的腫瘍送
達の F-SL に対する影響が異なる可能性や，F-SL
は腫瘍集積後，葉酸受容体による取り込みにより薬
効が高まったと推察された．以上より，A-83-01
は抗がん薬封入微粒子の腫瘍集積性を高め，抗腫瘍
効果を増強することが明らかとなった．

7. おわりに

　これまでに，1）Gd-L を用いた DCE-MRI は，
腫瘍の血管透過性と，腫瘍への微粒子製剤送達の評
価に有用である，2）MRI による ADC 値の取得
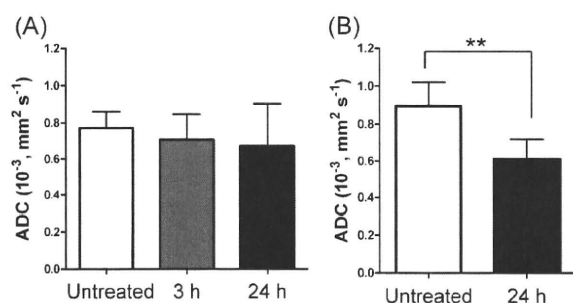は，造影剤を使用せずに容易に腫瘍の微小環境変化
を評価できる，3）DCE-MRI ガイド下で腫瘍微小

Fig. 5.　Apparent Diffusion Coefficient（ADC）of the Colon 26 Tumors before and at 3 h or 24 h after Single（A）and Repeated（B）A-83-01 Injection
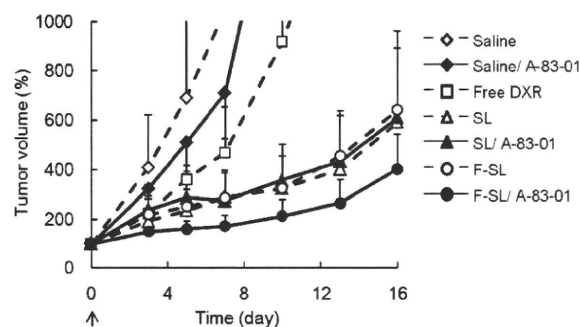　Each value represents the mean±S.D.（$n=4$）．**$p<0.01$

Fig. 6.　Effects of A-83-01 on the Antitumor Activity of Liposomal Doxorubicin（DXR）in Mice Bearing M109 Tumors
　Free DXR, PEGylated liposomal DXR（SL）, or folate-linked SL（F-SL）at 8 mg/kg body weight was administered intravenously with or without intraperitoneal A-83-01 injection. Each value represents the mean±S.D.（$n=6\text{--}8$）．

REFERENCES

1) Matsumura Y., Maeda H., *Cancer Res.*, **46**, 6387–6392 (1986).

2) Li C. J., Miyamoto Y., Kojima Y., Maeda H., *Br. J. Cancer*, **67**, 975–80. (1993).

3) Seki T., Fang J., Maeda H., *Cancer Sci.*, **100**, 2426–2430 (2009).

4) Kano M. R., Bae Y., Iwata C., Morishita Y., Yashiro M., Oka M., Fujii T., Komuro A., Kiyono K., Kaminishi M., Hirakawa K., Ouchi Y., Nishiyama N., Kataoka K., Miyazono K., *Proc. Natl. Acad. Sci. USA*, **104**, 3460–3465 (2007).

5) Tojo M., Hamashima Y., Hanyu A., Kajimoto T., Saitoh M., Miyazono K., Node M., Imamura T., *Cancer Sci.*, **96**, 791–800 (2005).

6) Morgan B., Thomas A. L., Drevs J., Hennig J., Buchert M., Jivan A., Horsfield M. A., Mross K., Ball H. A., Lee L., Mietlowski W., Fuxuis S., Unger C., O'Byrne K., Henry A., Cherryman G. R., Laurent D., Dugan M., Marme D., Steward W. P., *J. Clin. Oncol.*, **21**, 3955–3964 (2003).

7) Tofts P. S., *J. Magn. Reson. Imaging*, **7**, 91–101 (1997).

8) Ewing J. R., Knight R. A., Nagaraja T. N., Yee J. S., Nagesh V., Whitton P. A., Li L., Fenstermacher J. D., *Magn. Reson. Med.*, **50**, 283–292 (2003).

9) Patlak C. S., Blasberg R. G., Fenstermacher J. D., *J. Cereb. Blood Flow Metab.*, **3**, 1–7 (1983).

10) O'Connor J. P., Jackson A., Parker G. J., Jayson G. C., *Br. J. Cancer*, **96**, 189–195 (2007).

11) Daldrup-Link H. E., Okuhata Y., Wolfe A., Srivastav S., Oie S., Ferrara N., Cohen R. L., Shames D. M., Brasch R. C., *Microcirculation*, **11**, 387–396 (2004).

12) Daldrup H., Shames D. M., Wendland M., Okuhata Y., Link T. M., Rosenau W., Lu Y., Brasch R. C., *AJR Am. J. Roentgenol.*, **171**, 941–949 (1998).

13) Minowa T., Kawano K., Kuribayashi H., Shiraishi K., Sugino T., Hattori Y., Yokoyama M., Maitani Y., *Br. J. Cancer*, **101**, 1884–1890 (2009).

14) Jain R. K., *Science*, **307**, 58–62 (2005).

15) Tong R. T., Boucher Y., Kozin S. V., Winkler F., Hicklin D. J., Jain R. K., *Cancer Res.*, **64**, 3731–3736 (2004).

16) Taniguchi Y., Kawano K., Minowa T., Sugino T., Shimojo Y., Maitani Y., *Cancer Sci.*, **101**, 2207–2213 (2010).

The Impact of Thermal Treatment on the Stability of Freeze-Dried Amorphous Pharmaceuticals: II. Aggregation in an IgG1 Fusion Protein

BINGQUAN WANG,[1] MARCUS T. CICERONE,[2] YUKIO ASO,[3] MICHAEL J. PIKAL[1]

[1] Department of Pharmaceutics, School of Pharmacy, University of Connecticut, Storrs, Connecticut 06269

[2] Polymers Division, National Institute of Standards & Technology, Gaithersburg, Maryland 20899

[3] National Institute of Health Sciences, 1-18-1 Kamiyogo, Setagaya, Tokyo 158-8501, Japan

ABSTRACT: The objective of this research was to investigate the impact of thermal treatment on storage stability of an IgG1 fusion protein. IgG1 protein formulations were prepared by freeze-drying the protein with sucrose. Some samples were used as controls, and others were subjected to a further heat treatment (annealing). The protein structure was investigated with Fourier transform infrared spectroscopy (FTIR), and protein aggregation was monitored with size exclusion HPLC. Enthalpy recovery was studied using DSC, and global mobility represented by the structural relaxation time constant (τ^β) was characterized by a thermal activity monitor (TAM). The local mobility of the protein system was monitored by both ^{13}C solid-state NMR and neutron backscattering. Annealing increased the storage stability of the protein, as shown by the smaller aggregation rate and less total aggregation at the end of a storage period. The structural relaxation time constant of an annealed sample was significantly higher than the unannealed control sample, suggesting a decrease in global mobility of the protein system upon annealing. However, annealing does not significantly impact the protein secondary structure or the local mobility. Given the similar protein native structure and specific surface area, the improved stability upon annealing is mainly a result of reduced global molecular mobility. © 2009 Wiley-Liss, Inc. and the American Pharmacists Association J Pharm Sci 99:683–700, 2010

Keywords: annealing; physical aging; freeze drying/lyophilization; molecular mobility; global dynamics (α relaxation); local dynamics; enthalpy relaxation; pre-T_g endotherms; enthalpy recovery; protein structure; pharmaceutical stability; protein aggregation; IgG1 protein

INTRODUCTION

Stabilization of protein therapeutics is important for efficacious treatments for human diseases and conditions. One of the most effective methods for stability improvement is to freeze dry these biologicals with a stabilizer such as sucrose or trehalose,[1,2] and the obtained products may have a shelf life of 18–24 months, which is typically required for economic viability.[3,4] However, the cold chain requirement of storage condition may

limit the availability of biopharmaceuticals to developing countries. Also the bioshield project (http://www.whitehouse.gov/infocus/bioshield/) proposes a longer shelf life (~10 years) for "next-generation" drugs including vaccines. In order to meet these requirements, strategies other than the traditional formulation methods are desired to further improve the stability of biopharmaceuticals.

Recently, it was reported that the stability of amorphous solids is also dependent on the process used to prepare the material, with "thermal history" being one critical factor.[5-7] Thus, the drying processes with different thermal histories may impact the stability of pharmaceuticals.[6,9] Glass dynamics have been proposed as an important factor in the stabilization effect of amorphous excipients on proteins during drying and storage[10,11] This mechanism states that the excipient forms a rigid matrix in which the protein is molecularly dispersed, and the limited mobility in the high viscosity glass slows down the protein mobility which is necessary for protein degradation. According to the Stokes–Einstein equation, the diffusion coefficient in supercooled liquid is inversely proportional to the viscosity of the system.[12] Structural relaxation time, a measure of molecular mobility, is also related to the diffusion coefficient.[11,12] Thus, chemical reactions that require diffusion can have a dependence on molecular mobility or structural relaxation time of the system.

DSC and other calorimetry studies suggest that a correlation does exist between chemical instability and the structural relaxation time of the amorphous system.[13-19] For example, Duddu et al.[17] reported the correlation of aggregation of an IgG1 antibody with the reduced time (t/τ) below T_g. Shamblin et al.[18] reported strong coupling between the dimerization rate of etha-crynate sodium (ECA) and structural relaxation time in formulations colyophilized with sucrose, trehalose, and PVP. Recently, it was found that there is a correlation between the rate of degradation and structural relaxation time in human growth hormone (hGH) protein systems lyophilized with several sugars.[19] However, it is also noticed that there are reports in pharmaceutical literature that provide examples of a poor correlation. The contribution of molecular mobility was found to be small in insulin degradation in trehalose formulations under high humidity conditions,[20] as well as with PVP.[21] Therefore, while there are numerous examples of a correla-

tion between structural relaxation and reactivity, the correlations may not always be strong.

Thermal treatment of dried glass results in an increase in the structural relaxation time (or decrease in global mobility). A glass is in a non-equilibrium state and it exhibits higher enthalpy, free energy, and entropy than the corresponding equilibrium supercooled liquid. Due to its higher energy, a glass will relax toward the equilibrium curve in an experimentally accessible timescale if there is sufficient mobility. The process of relaxation toward equilibrium is known as physical aging or annealing.[22] In this article, we use "annealing" to describe a process wherein an amorphous material is kept at a temperature below T_g for a period of time sufficient to allow significant relaxation toward the equilibrium state. During the annealing period, some physical and mechanical properties of amorphous solid will change with time. For example, the time-dependent changes in glassy polymers upon annealing include increase in density, yield stress, and decreases in stress relaxation rate, free volume, and enthalpy.[22,23] For our interests, the primary effect of annealing of amorphous glass is the increase in structural relaxation times and thus reduction in global mobility.[8,22,23]

If chemical/physical stability and structural relaxation time are coupled in a glass, then a sample with a larger structural relaxation time resulting from annealing should have better stability. That is, stabilization against pharmaceutical degradation could be achieved by annealing for a short period of time. There are several studies supporting the concept of "stabilization by annealing" in both the food and the pharmaceutical literature. The first demonstrated example of stabilization of pharmaceuticals by annealing involved an antibacterial (moxalactam disodium) formulation colyophilized with 12% (w/w) mannitol.[24] Drying of the antibacterial system (with a T_g about 121°C) using 60°C instead of 40°C during the secondary drying process gave samples of essentially identical residual moisture but the higher temperature drying protocol gave a systematic improvement in storage stability that averages about 20%. This system was further investigated, and the stabilization effect was correlated to the reduced molecular mobility.[25] Hill et al.[5] studied the annealing effect in food systems, and the rate of Maillard reaction between lysine and glucose was found to be about 20% slower in the aged glassy matrix after aging for 3 weeks at a temperature of 30°C below T_g.

Luthra et al.[26] reported that rate of cyclization degradation reaction in aspartame/disaccharide glass decreases significantly when the freeze-dried sample was heat treated postlyophilization in an oven. Recently, it was found that annealing resulted in the decrease in dimerization rate of ECA, and thus annealing can also stabilize intermolecular degradation reactions that involves mobility on longer length scales such as dimerization processes.[27] While these observations show that thermal treatment may be used to increase the long-term stability, evidence for this stabilization effect on amorphous pharmaceuticals is still limited. Furthermore, these annealing studies only focused on small molecule pharmaceuticals, and the consequence of annealing on delicate large protein molecules is unknown. Given the desire to improve the stability of biologics, it will be very important to determine if protein biopharmaceuticals can also be stabilized by annealing.

In this article, the impact of annealing on the stability of an IgG1 fusion protein is investigated. Previous studies showed that the stabilization effect from sugar is dependent on the disaccharide level, and a formulation with higher sucrose level generally exhibited much better storage stability.[19,28,29] However, a protein formulation with higher sugar level is not always practical due to limits imposed by the disease state (such as diabetes) or manufacturing constraints (such as long lyophilization cycle due to high solid content associated with high sucrose level). Here, low sugar content formulations would be preferred if sufficient stability can be obtained, for example, by annealing. We have chosen two formulations with low-to-moderate sugar level (sucrose/IgG1 protein mass ratio of 0.5 and 1) in this study and have conducted an extensive investigation of the impact of annealing on selected physical properties, protein structure in the solid, molecular mobility, and aggregation stability.

EXPERIMENTAL

Materials

A recombinant humanized IgG1 fusion protein with a molecular weight of 185 kDa was provided by Wyeth Biopharma (Andover, MA). The protein drug substance was ultrafiltered through a regenerated cellulose membrane filter (Billerica, MA, area of 50 cm^2, 30 kDa molecular weight cutoff

value).[1] The L-histidine, sodium chloride, poly-L-lysine, 2-hydroxylpropyl-β-cyclodextrin, pluronic F68 (a hydrophilic nonionic surfactant), polysorbate-80, and glycine were purchased from Sigma (St. Louis, MO). α-Sucrose with reduced heavy metal (<5 ppm) content was purchased from Calbiochem of EMD Biosciences (San Diego, CA). These reagents were of the highest grade available and were used without further purification.

Lyophilization Procedures

Ten milligrams per milliliter IgG1 protein solutions were prepared after dialysis against two buffer solutions: one buffer was 1 mM histidine buffer (pH 6.5), and another was 1 mM histidine buffer and 40 mg/mL of sucrose (pH 6.5). By mixing two stock solutions at different ratios, two protein formulations with sucrose/IgG1 protein mass ratios of 0.5 and 1 were prepared. The formulation with sucrose/IgG1 protein mass ratios of 0.5 and 1 is defined as P10S5 and P10S10, respectively, where P represents the protein, S represents sucrose, and the number is the concentration (mg/mL) of the component in the formulation.

Protein solutions (1 mL) were filled into 2 mL tubing glass vials and were lyophilized in a Genesis 25 EL (SP Industries, Gardiner, NY) freeze-dryer. The samples were first dried at a shelf temperature of −25°C with a chamber pressure of 6.6 Pa (50 mT) for 20 h, and then the samples were further dried at about 4 Pa (30 mT) with a shelf temperature of −25°C for 35 h. Primary drying was conducted below the glass transition temperature of freeze-concentrate (T'_g) of both formulations. Secondary drying was carried out for 6 h at 25°C. After the drying process was finished, vials were stoppered under dry nitrogen with Daikyo Flurotec stoppers (West Pharmaceutical, Lititz, PA) and capped with aluminum seals. All the samples were amorphous after freeze-drying as evidenced by the absence of birefringence with polarized light microscopy (PLM; Linkam, McCrone, Chicago, IL).

Residual Water Measurement

The water content for each formulation after freeze-drying was determined using Metrohm

Karl Fischer coulometer (Riverview, FL). At least two vials of each sample were used. Freeze-dried sample vials were reconstituted in 2 mL dried methanol and 0.5 mL of the solution was injected into the titrator. Blank corrections were applied. Standard deviation from replicate measurements was less than 0.2% (w/w).

Specific Surface Area Measurement

Specific surface area (SSA) analysis was performed using a FlowSorb II 2300 surface area analyzer (Micromeritics, Norcross, GA). A protein sample of about 100 mg was loaded into the sample holder in the glove bag with controlled humidity (<2%). Single point calibration was performed prior to taking surface area measurements using 1 mL Krypton gas. Powder samples were degassed for at least 3 h at 35°C in the Flow Prep oven, and surface areas were measured using krypton (Kr) as an adsorbate and helium as carrier.

Differential Scanning Calorimeter (DSC) Measurements

Modulated DSC (Q1000; TA Instruments, New Castle, DE) was used to measure the glass transition temperature (T_g) and the change in heat capacity at T_g (ΔC_p) of protein samples. The samples were run at a 2°C/min heating rate, modulated with a ±1°C amplitude every 120 s. Fresh protein samples with sucrose/protein mass ratios of 0.5 and 1 give T_g of 106 and 101°C (mid-points), respectively.

Enthalpy recovery (ΔH) of the annealed sample was measured using standard (nonmodulated) DSC following the previously described procedure.[27] The scan rate used was 10°C/min. Briefly, the heating curve of the first DSC scan was used to obtain the area of the endothermic recovery peak by integration using Universal Analysis Software (TA Instruments). The thermal history of the annealed sample was then erased by holding the sample at a temperature above T_g, the sample was cooled, and a second DSC curve was obtained, representing zero annealing time. The second scan curve is given in Figure 1. We define the enthalpy recovery (ΔH) as the enthalpy difference between the annealed sample and the sample with erased thermal history.

The relaxation enthalpy at infinite time (ΔH_∞) at a given annealing temperature (T_a) was
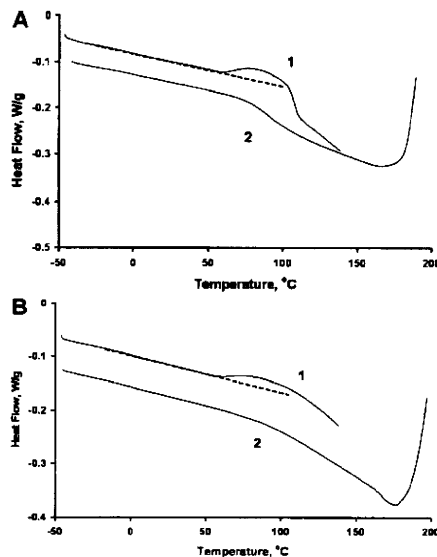

Figure 1. DSC of a fresh IgG1/sucrose sample showing the exothermic pre-T_g peak in the P10S10 formulation (A) and P10S5 formulation (B). The dashed line in the first scan (curve 1) is added to guide the eye to differentiate the pre-T_g event. The second scan after eliminating the thermal history (curve 2) showed the disappearance of pre-T_g event. The lines were offset for clarity.

calculated using the following equation:[30,31]

$$\Delta H_\infty = (T_g - T_a) \times \Delta C_p \qquad (1)$$

A relaxation function (Φ) served as a measure of the extent of enthalpy relaxation during annealing and was calculated as follows:[31–33]

$$\Phi = 1 - \frac{\Delta H}{\Delta H_\infty} \qquad (2)$$

where ΔH is the enthalpy recovery measured from DSC and ΔH_∞ is the corresponding value at time infinity as obtained from Eq. (1).

Structural Relaxation Time Measurement by Thermal Activity Monitor

Isothermal microcalorimetry was used to measure the rate of enthalpy relaxation of the sample at the storage temperature (50°C) using a Thermometric, 2277 Thermal Activity Monitor (Thermo-

metric, Jarfalla, Sweden). The experimental procedure and data analysis using Kohlraush–Williams–Watts (KWW) curve fitting is similar to that described in a previous report.[27]

Studies of Protein Aggregation by Size Exclusion Chromatogram

Assay for chemical degradation was not routinely performed because the protein samples did not show sufficient chemical degradation to allow a quantitative analysis of chemical instability. Size exclusion chromatography (SE-HPLC) was used to assess the physical aggregation of the protein during storage. The initial SE-HPLC assays were run on both fresh samples (nonannealed) and on samples exposed to different annealing conditions. The rest of the sample vials were then transferred to an oven at 50°C. After storing for preset times (0.5, 1, 3, and 6 months), the samples were reconstituted with 1 mL of purified water. All solutions obtained were visually clear after reconstitution, and the soluble protein aggregate was analyzed with HPLC.

A column of YMC DL20S05-3008WT (Waters, Milford, MA) was used with a flow rate of 1 mL/min. The mobile phase consisted of 0.02 mol/L NaH_2PO_4 and 0.2 mol/L NaCl (pH 7.2). UV absorption was monitored at 280 nm. The dimer eluted at about 6.2 min and the monomer peak appeared at about 6.8 min. The standard error in the percentage of aggregate for all sample replicates was <0.5%.

To evaluate the effect of variable diluent composition on the measured aggregation, reconstitution of lyophilized protein formulations was also carried out using reconstitution media containing 0.5% (w/w) additives such as phosphate buffer, dextran sulfate, 2-hydroxylpropyl-β-cyclodextrin, pluronic F-68, and polysorbate-80. Then, the amount of aggregate in the reconstituted sample was measured by SE-HPLC analysis.

Protein Structure Characterization by FTIR

Fourier transform infrared spectroscopy (FTIR) studies were conducted using a Nicolet Magna-IR 560 spectrometer (Thermo Electron, Madison, WI). The study was carried out using transmission mode on the freeze-dried protein solids according to procedures in the literature.[34,35] A total of 128 scans and 4 cm^{-1} resolution were used for each spectrum. About 2 mg of solid protein sample was mixed with 200 mg dried KBr powder, and the mixtures were then pressed with a Carver press at 11,000 psi for about 2 min. The obtained transparent pellet was put into the sample holder and then loaded into a dried air-purged measurement chamber. The protein spectrum was collected and the absorbance signal was obtained using the corresponding background. Second derivative spectra were then obtained using an OMNIC software. The second derivative of the amide I region (1700–1600 cm^{-1}) of the spectra was baseline corrected and area normalized. The peak height of the major band was used to compare the similarity between spectra.

Fast Local Dynamics from a Neutron Backscattering Spectrometer

The fast local dynamics with timescale of nanoseconds was studied with a high flux backscattering (HFBS) spectrometer at the Center for Neutron Research on the NG2 beam line at the National Institute of Standards and Technology (NIST).[36] Only those motions with timescales shorter than 5 ns can be measured with this instrument.[37] The details of the experimental procedure and data analysis have been published elsewhere.[27,38,39] A larger mean square of displacement of H-atom (msd, $\langle u^2 \rangle$) means a higher local mobility of the system.

Determination of $T_{1\rho}$ of Protein and Sucrose by ^{13}C Solid-State NMR

The rotating-frame spin-lattice relaxation time ($T_{1\rho}$) of the IgG1 carbonyl carbon in lyophilized protein/sucrose formulations was determined at 25°C using a UNITY plus spectrometer (Varian, Inc., Paulo Alto, CA) operating at a proton resonance frequency of 400 MHz. Spin-locking field was equivalent to 19 kHz. The rotor size was 7 mm and spinning speed was 4 kHz. Peak height at about 180 ppm due to IgG1 carbonyl carbon and 80 ppm from sucrose were followed with different delay times.[40] Similar measurement of $T_{1\rho}$ was performed for annealed protein samples. The data were fit to a biexponential decay model to determine the two $T_{1\rho}$ as reported elsewhere for freeze-dried systems.[40,41] Since the shorter $T_{1\rho}$ value was the same for all samples, the longer $T_{1\rho}$ values were used for comparison between samples annealed at different conditions.

RESULTS AND DISCUSSIONS

Impact of Annealing on Physical Properties of IgG1 Protein Samples

Annealing appeared to have no impact on the physical form or the SSA of the protein samples we studied. The fresh unannealed and annealed samples were confirmed to be amorphous by PLM. Even upon storage at 50°C for 6 months, we observed no crystallization of sucrose by PLM. Sample SSA was also unaffected by annealing. For the fresh unannealed sample, the SSA was approximately $1.7 \pm 0.2\,m^2/g$, which is similar to that reported for other protein pharmaceuticals.[6,42] After annealing at 70°C for 20 h, the most aggressive annealing protocol we used, the SSA of the aged sample was essentially unchanged at $1.9 \pm 0.1\,m^2/g$. This result was consistent with previous reports that aging did not lead to perceptible changes in morphology or particle size in a trehalose system.[43]

The impact of annealing on residual moisture of the protein sample was determined with Karl Fischer titration (Tab. 1). The fresh protein sample immediately after freeze drying showed low moisture level (about 0.5%, w/w). Upon annealing of protein samples at high temperatures for 10 or 20 h, the residual water increased by 0.5–1%. In addition, upon storage at 50°C for 3 months, all samples, fresh and annealed, showed a moisture level of about 2% (w/w). The increase in the moisture upon annealing or storage is believed due to the transfer of moisture from the stopper to the dried cake.[44–46] Even though there are changes in moisture during annealing, these small changes are not expected to significantly impact enthalpy relaxation and stability. In

Table 1. Percent Residual Water Content (%) in P10S5 Sample upon Annealing at Different Conditions

Sample	Initial Sample (T_0)	Stored at 50°C for 3 Months
Fresh	0.5 ± 0.06	2.0 ± 0.2
An60d10h	1.0 ± 0.06	2.4 ± 0.2
An60d20h	1.0 ± 0.21	n/d
An70d10h	1.4 ± 0.06	2.3 ± 0.08
An70d20h	1.6 ± 0.32	n/d
An80d10h	1.4 ± 0.07	2.4 ± 0.16

n/d, not determined.
Standard error shown is based on three replicates. The term "An60d10h" means that the sample was annealed at 60°C for 10 h.

similar protein systems, changes in moisture from 0% to 3% showed only very slight changes in stability.[47] Also in previous peptide/sugar and ECA/sugar systems where there were large total sample amounts in a vial, no obvious changes in moisture were observed upon annealing, even though annealing caused significant changes in enthalpy relaxation.[26,27] In short, there is significant precedent for annealing causing increases in relaxation time and stabilization, even if not in protein systems, so the results obtained in this study are consistent with previous results. In addition, we note that the structural relaxation time increases sharply upon annealing as shown below from the TAM experiments, so the water plasticization effect on global molecular mobility is obviously overwhelmed by the annealing effect itself, so the impact of water content variations such as those shown in Table 1 on relaxation dynamics and stability is not expected to be significant.

DSC Investigation of Pre-T_g Event and Enthalpy Recovery

Pre-T_g exothermic events have been reported for freshly freeze-dried glasses;[27,48–50] and here we investigated this phenomenon by DSC. The IgG1/sucrose formulations were scanned from about $-50°C$ to a temperature above T_g. Figure 1 shows the DSC curves of fresh P10S10 (T_g of 101°C) and P10S5 (T_g of 106°C) formulations, which were dried for 6 h at 25°C in secondary drying. Notice that pre-T_g exothermic peaks were observed at about 60°C in both protein formulations in the first scan. To investigate the source of the pre-T_g peak in the fresh sample, the DSC sample was kept at a temperature of about 30°C above T_g for 5 min to erase the thermal history of the glass, and then cooled down to $-50°C$ and rescanned. The second scan showed a typical glass transition, with a clear absence of a pre-T_g exothermic peak in both formulations.[48,50] This suggests that the pre-T_g event in the freshly lyophilized sample is a result of the thermal history it experienced during the normal freeze-drying cycle.

The pre-T_g event in annealed protein samples was also investigated using DSC. The impact of annealing on DSC behaviors of P10S10 and P10S5 is shown in Figure 2. Upon annealing at low temperature, the pre-T_g exothermic peak converted to pre-T_g endothermic peak for both samples. Increasing the annealing temperature resulted
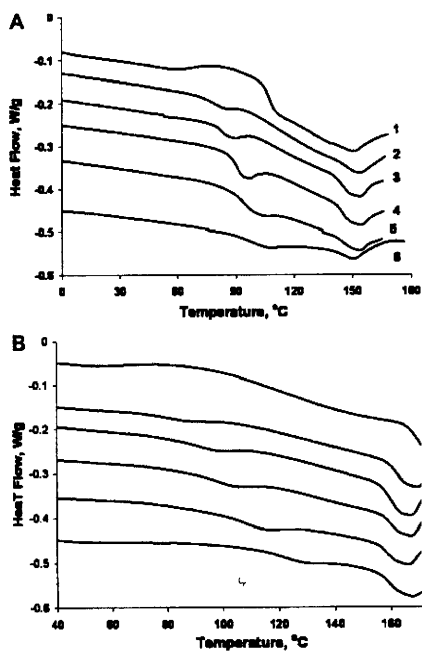
Figure 2. DSC curves of unannealed fresh IgG1/sucrose sample (curve 1) and samples annealed for 20 h at different temperatures. (A) P10S10 formulation annealed at 60°C (curve 2), 65°C (curve 3), 75°C (curve 4), 85°C (curve 5), and 90°C (curve 6). (B) P10S5 formulations annealed at 60°C (curve 2), 70°C (curve 3), 80°C (curve 4), 90°C (curve 5), and 105°C (curve 6). The endothermic thermal events around 150°C (P10S10) and 170°C (P10S5) are likely denaturation endotherms while the thermal events at lower temperatures represent T_g and relaxation events.

peaks are associated with a very broad distribution of the structural relaxing populations.[8,48,50–52,54] It is possible that some relaxing species may have relaxation times shorter than the annealing time at the annealing temperature, and thus they have relaxed during the annealing step.[48] Upon reheating the sample during the DSC scan, these fast relaxing species may regain the lost energy which then results in the formation of a pre-T_g endotherm.[27]

The enthalpy relaxation upon annealing was studied as a function of annealing time and temperature. For relaxation studies using DSC, it is assumed that the enthalpy relaxation that occurred during the annealing process is identical to the enthalpy recovery measured during the heating scan in DSC. Here, enthalpy recovery was determined by integration of the endothermic peak with a sigmoidal baseline feature, as discussed in the Experimental Section. Figure 3 shows the impact of annealing temperature on the enthalpy recovery of IgG1/sucrose formulations. The magnitude of enthalpy recovery increased upon increasing the aging temperature initially. However, a maximum enthalpy recovery was observed at about 85°C for the P10S10 formulation, and further increases in annealing temperature produced a decrease in the enthalpy recovery. Similarly, a maximum enthalpy recovery is observed at about 90°C for the P10S5 formulation. Thus, both formulations give a maximum
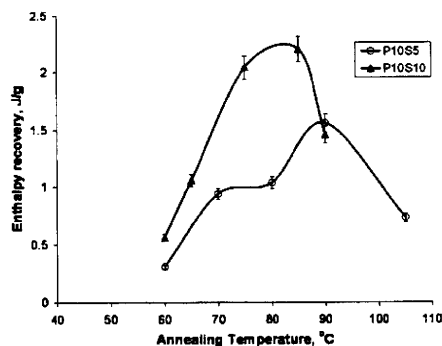
in the shift of the endothermic peak to a higher temperature, and finally the peak appeared as a T_g overshoot. The physical basis of the pre-T_g events is not well understood even though these events have been reported elsewhere.[47,48,51–53] Our studies show that annealing significantly impacts pre-T_g events, but as discussed below, we observe no impact of annealing on β relaxation, either as measured by neutron scattering or by NMR. Thus, it seems that pre-T_g event is not a result of β relaxation motions. Presumably these

Figure 3. Impact of annealing temperature on the enthalpy recovery of IgG1/sucrose formulations after annealing for 20 h. Note the enthalpy recovery reaches a maximum for both protein formulations at about 15°C below T_g. Error bars are standard errors for 2–3 replicates.

enthalpy recovery at about 15°C below their T_g, which is expected based on previous studies.[27,48]

The impact of annealing time on enthalpy recovery was also investigated. The enthalpy recovery was found to be proportional to the log of annealing time (results not shown), which is consistent with previous report on small pharmaceutical molecules.[26,27] The logarithmic dependence of enthalpy on annealing time means that the enthalpy relaxes much more rapidly in the short time range than at longer times. Density studies from this laboratory (unpublished) on the pure trehalose system also showed that the density increase (or free volume decrease) is most pronounced early in the annealing process (for about 5–10 h). Thus, for the application of annealing to lyophilization cycle development, the annealing time has been selected to be 10 or 20 h in our study.

Figure 3 shows that P10S10 give larger enthalpy recovery than P10S5 upon annealing at the same conditions (60°C for 20 h). Also the P10S10 sample annealed at 75°C exhibited higher enthalpy recovery than the P10S5 sample annealed at 80°C for the same periods of time. Therefore, it seems that the protein formulation with higher sucrose fraction shows higher enthalpy recovery than the protein formulation with lower sucrose level. This observation is a direct result of Eq. (1) and the larger ΔC_p for a system richer in sucrose. As a strong glass, a pure protein exhibits a very broad T_g with a very small heat capacity change, ΔC_p, which makes it difficult or impossible to measure the T_g of pure proteins with DSC.[50] In contrast, sucrose is a fragile glass and exhibits large ΔC_p at T_g, and thus the enthalpy relaxation in sucrose is much larger than in a protein according to Eq. (1).

Investigation of the Impact of Annealing on the Storage Stability of IgG1

In order to determine if the reconstitution process will impact the measured aggregation, the effect of reconstitution media on the amount of protein aggregate measured was studied. Table 2 shows the aggregate level in the IgG1 protein formulation upon reconstitution in fresh and annealed samples. We note that the addition of surfactant or polyanions did not significantly impact the amount of aggregation measured. Similar observations have been made for some other proteins.[39,40] Thus, for the systems studied in this research, the reconstitution process did not significantly impact aggregate formation. We thus conclude that stability differences of the IgG1 protein upon annealing are mainly the result of the bimolecular aggregation events that actually occur in the solid-state during storage. That is, development of aggregation that correlates with storage time and conditions could reflect a bimolecular aggregation event that occurs during storage or could reflect time-dependent protein structural alteration during storage, with the actual aggregation event occurring mostly during reconstitution when molecular mobility becomes very high. For our systems, the role of aggregation during reconstitution is, at best, minimal.

The time dependence of IgG1 aggregation upon storage at 50°C was studied for both protein formulations. As shown in Figure 4A, the fresh sample of the P10S10 formulation showed less degradation than the annealed sample at time 0, as expected because some degradation will occur during annealing. However, upon storage for about 1 month, these samples showed almost identical aggregate level, and further storage for

Table 2. Effects of Reconstitution Medium on the Amount of Protein Aggregation Measured in the P10S5 Formulation upon Lyophilization and Storage at 50°C

Reconstitution Medium	Immediately After Freeze Drying	Anneal at 50°C for 7 Days
Water	5.5 (0.32)	8.8 (0.17)
Phosphate buffer	5.6 (0.27)	9.0 (0.14)
Dextran sulfate	5.8 (0.14)	9.1 (0.18)
2-hydroxylpropyl-β-cyclodextrin	5.8 (0.16)	8.9 (0.04)
Pluronic F-68	5.5 (0.18)	8.8 (0.12)
Tween-80	5.3 (0.20)	8.7 (0.11)

5% additives unless specified otherwise.
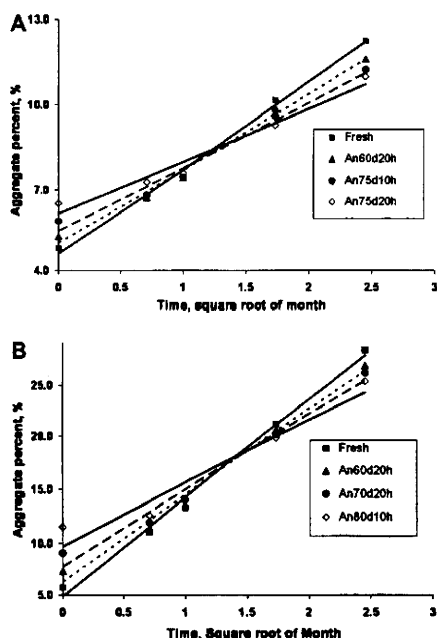Values in brackets represent standard deviation ($n = 6$).

Figure 4. Time dependence of IgG1 aggregation upon storage at 50°C for P10S10 (A) and P10S5 formulation (B). Note the linear relationship between the protein aggregation and square root of time in the x-axis. The correlation coefficients for P10S10 are 0.995, 0.991, 0.987, and 0.968 with increasing annealing temperature. The regression coefficient for P10S5 is 0.993, 0.989, 0.979, and 0.937 with increasing annealing temperature. The slope of the best-fit straight line is used as the degradation rate constant. The error bars are about the size of the symbol.

longer times resulted in the annealed sample having less aggregation. That is, the annealed sample not only showed a lower degradation rate during storage (i.e., smaller slope), but in spite of the degradation suffered during annealing, actually exhibited less total degradation at the end of storage than the fresh sample. These data (Fig. 4A) are an excellent example of large differences in stability that can result from annealing. Similar to the P10S10 formulation, annealing also stabilizes the protein-rich P10S5 formulation as shown in Figure 4B. Again, annealed samples exhibited lower total aggregate

levels after storage for more than about 2 months. Thus, our postulate that protein systems can be stabilized by annealing is valid for both IgG1 formulations.

The protein aggregation kinetics in freeze-dried solids were evaluated and these stability data were found to fit square root of time model best, as measured by a high correlation coefficient.[27] The correlation coefficients, as shown in Figure 4, are still relatively high enough even though they do seem to decrease upon increasing annealing temperature. Since the fit to square root of time model was better than the first-order kinetics even for the annealed samples, the square root of kinetics was used throughout the article for consistency when comparing the storage stability of different samples. This square root of time degradation kinetics is commonly observed in glassy materials.[19,25–27,31,32] Therefore, the aggregation rate constants were obtained as the slope of the straight line in Figure 4. Table 3 shows the aggregation rate constants and initial aggregate levels of IgG1 protein at 50°C upon annealing at different conditions. The annealed P10S10 formulation had only slightly higher initial degradation in the annealed samples relative to the unannealed system (with initial aggregate range from 4.8% in fresh to 6.5% maximum in annealed), which is due to degradation occurring during the thermal treatment. In contrast, the P10S5 formulation gives a relatively large change in initial aggregate upon annealing at high temperature. Also, the P10S5 formulation gave a higher rate of degradation as compared to the P10S10 formulation with the same thermal history. The better stability in P10S10 than P10S5 is consistent with previous findings that a higher amount of sucrose in protein formulations can afford better protection to the protein in the glassy solid.[19,29,39] It was found that P10S10 formulation showed lower molecular mobility, lower free volume, and lower degree of native structure perturbation than P10S5,[39] all of which are consistent with the better stability in P10S10 than P10S5 upon annealing and storage.

The general trend in the physical stability data shows that as annealing temperature increased, long-term stability improved (i.e., the rate constant decreased). Therefore, annealing below T_g can slow down the aggregation rate of the protein. In spite of increased initial aggregation after the annealing process, annealed samples actually showed less aggregation after storage for 3 and 6 months (see Fig. 4). For P10S10, the control

Table 3. Initial Aggregation Level and Aggregation Rate Constants of IgG1 Protein/Sucrose Formulations at 50°C upon Annealing at Different Conditions

Annealing Temperature (°C)	Annealing Time (h)	Initial % Aggregation	k at 50°C
P10 S10 control (fresh)		4.8 ± 0.1	3.1 ± 0.1
60	10	5.1 ± 0.1	2.9 ± 0.1
60	20	5.3 ± 0.2	2.7 ± 0.1
65	10	5.4 ± 0.3	2.8 ± 0.2
65	20	5.6 ± 0.4	2.5 ± 0.2
75	10	5.8 ± 0.3	2.3 ± 0.2
75	20	6.5 ± 0.3	1.9 ± 0.2
P10 S5 control (fresh)		5.8 ± 0.2	9.4 ± 0.5
60	10	6.9 ± 0.3	8.8 ± 0.5
60	20	7.4 ± 0.3	8.2 ± 0.5
70	10	7.9 ± 0.4	7.6 ± 0.4
70	20	9.1 ± 0.3	7.2 ± 0.6
80	10	11.5 ± 0.3	6.0 ± 0.8
80	20	13.3 ± 0.4	5.6 ± 0.6

Uncertainties given for the rate constants are standard errors as provided by the regression analysis based on the square root of time kinetics.

(fresh) sample and sample annealed at 75°C for 20 h give degradation rate constants of 3.1 and 1.9, respectively. Thus, annealing results in a decrease in degradation rate constant of about 40% for IgG1 protein. Also the P10S5 sample annealed at 80°C gives similar improvement in stability. These data (Tab. 3 and Fig. 4) clearly demonstrate that annealing improves long-term stability of the IgG1 protein.

In order to further address the question "Does annealing significantly impact aggregation of IgG1 protein?," a statistical test using the general linear model (GLM) procedure was performed on the rate constant data to determine the effect of both annealing temperature and time. The GLM results for P10S5 data showed a significant contribution of both annealing time ($p = 0.088$) and annealing temperature ($p < 0.001$) on the differences observed in aggregation rate between control (fresh) and annealed samples. Similarly, annealing significantly improved the stability of the P10S10 sample. Therefore, both annealing time and temperature significantly impact the stability.[27] It should be pointed out that initial degradation level may need to be considered to address product quality in a broader sense, as, for example, if there is potential toxicity and/or immunogenicity due to the degradation product produced during annealing. In the current study, the initial aggregate level upon annealing is

relatively high due to the protein drug substance, formulations, and annealing conditions used, but it should be emphasized that the total aggregate level of the annealed sample is less than that for·the nonannealed sample after about 2 months into the stability study. Moreover, the amount of degradation during annealing is protein, formulation, and process dependent. For example, our unpublished results on rHSA systems showed that the initial aggregate upon thermal treatment at 65°C for 20 h was still <0.5%, and a similar stabilization effect was observed upon annealing. In this example, the annealing approach is obviously a practical procedure for improving stability.

Impact of Annealing on Protein Native Structure

Figure 5 shows the impact of annealing on the protein structure in the solid as determined by area-normalized FTIR spectra of the IgG1 formulations. The spectra are characteristic of IgG1 protein which has a predominance of β-sheet structure at 1641 and 1693 cm^{-1}. Figure 5 shows the FTIR spectra of P10S10 after annealing at 70°C for different periods of time. After annealing at 70°C for 10 h, the peak height at 1641 cm^{-1} was essentially the same as the fresh sample. Even a sample annealed at 70°C for up to 40 h showed no
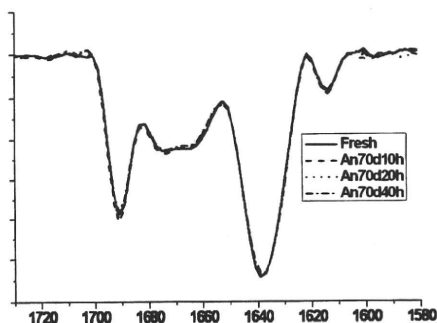
Figure 5. Area-normalized second derivative FTIR spectra of IgG1 P10S10 formulations after annealing at different conditions. Notice that no significant change in protein structure was observed upon high-temperature annealing. The data in the curve represent the average of three replicates.
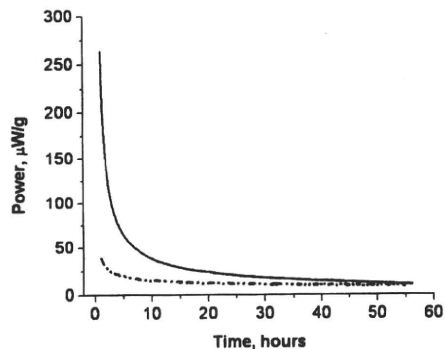

Figure 6. Power-time data at 50°C for a P10S10 sample annealed at 75°C for 10 h (dashed line) and fresh control sample (solid line). Note the higher power in the fresh sample than the annealed sample at same time, which indicates that annealed sample has a much lower molecular mobility.

obvious change in the amide I band. The same qualitative result has been observed for the P10S5 formulation (data not shown). These results indicate that no significant differences in the secondary structure of the protein are produced upon annealing for either formulation, at least within the sensitivity of the technique. The tertiary structure of the IgG1 upon reconstitution was also studied using fluorescence spectroscopy, and it was found that there was no significant shift in the emission peak maximum for both tyrosine and tryptophan residues upon annealing of P10S10 at 65°C for 10 h (data not shown). Of course, this does not mean changes in tertiary structure did not exist in the solid but simply "refolded" upon reconstitution. Since methodology suitable for characterization of tertiary structure in the glassy is not available, we studied secondary structure by FTIR. As indicated above, no changes in secondary structure upon annealing were observed. These results are consistent with recent observation that thermal denaturation of hGH in a glassy solid occurs only well above T_g.[55] FTIR, HPLC, and DSC results indicated that brief exposure of hGH to temperatures slightly less than the onset denaturation temperature in dried solid (i.e., below 150°C) did not cause significant damage to the protein.[55] These results suggest that thermal treatment of dry solids at a temperature well below T_g does not cause significant change of protein native structure.

Impact of Annealing on the Global Mobility

The rate of enthalpy loss was monitored using isothermal microcalorimetry. Figure 6 compares the thermal activity versus time curves at 50°C for control and annealed P10S10 samples. The thermal activity of the both samples decreases rapidly in the first 10 h, and then decreases slowly. This relaxation behavior is normally observed and is due to structural heterogeneity in the system.[8,33] It is widely accepted that a glass consists of a collection of "substates" with different sizes and entropies, each relaxing independently at different rates, giving rise to a broad distribution of structural relaxation times.[33,51,56] Also note (Fig. 6) that the annealed protein sample shows a very small heat flow signal compared to the

Table 4. Structural Relaxation Time Constant (τ^β) of P10S10 Sample at 50°C With Different Thermal Histories

Annealing Temperature (°C)	Annealing Time (h)	
	10	20
Fresh control	2.3 ± 0.6	
60	42 ± 3	49 ± 9
65	48 ± 5	41 ± 5
75	45 ± 4	52 ± 6

The τ^β value was calculated based on fitting of TAM data to the KWW model. The uncertainty is the standard error based on 2–3 replicates.

unannealed control sample. The effect of annealing conditions on the structural relaxation parameters of P10S10 is shown in Table 4. All annealed samples showed a large decrease in molecular mobility, as shown by the large increase in τ^β value from 2.3 for the control sample to about 40–50 after annealing. This decrease in global mobility upon annealing is caused by the post-lyophilization annealing process. The substates with small relaxation times are depopulated during annealing, leaving behind the populations with longer relaxation times. Therefore, annealing results in the increase in the relaxation time constant (i.e., a decrease in molecular mobility), as expected.

Local Dynamics Measurement by Neutron Scattering and Solid-State NMR

The effects of annealing on local motions with timescales much shorter than global motions were also investigated. The fast local mobility with a timescale of <5 ns was investigated with neutron backscattering, and the mean-squared displacement ($\langle u^2 \rangle$) of the hydrogen atomic motion was recorded at temperatures ranging from 40 to 330 K. Table 5 shows the $\langle u^2 \rangle$ of the P10S10 samples with different thermal histories at 25, 40, and 50°C. $\langle u^2 \rangle$ values increase monotonically with temperature for both samples, which reflects the higher mobility of the sample at higher temperature. However, there is no significant difference in the $\langle u^2 \rangle$ of the control (fresh) sample and the sample annealed at 60°C for 10 h at any temperature studied. Thus, it seems that the annealing does not significantly impact the fast local mobility in the protein/sucrose system, at least for the annealing conditions studied. This finding is consistent with the previous neutron backscattering study on ECA system with ECA/sugar mass ratio of 1:10.[27] Even upon moderate to strong

Table 5. Fast Local Mobility ($\langle u^2 \rangle$) of the P10S10 Sample Studied With Neutron Backscattering at Temperature of 25, 40, and 50°C

T (°C)	Fresh	An6010h
50	0.297 ± 0.005	0.286 ± 0.006
40	0.284 ± 0.006	0.273 ± 0.005
25	0.264 ± 0.006	0.253 ± 0.005

Standard error shown is the uncertainty in the best fit of data to a Debye–Waller harmonic model.
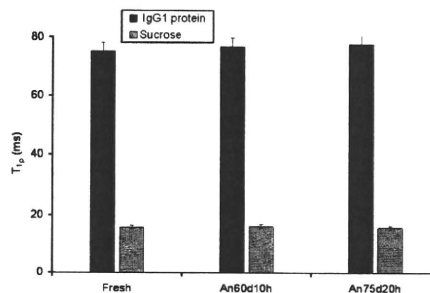

Figure 7. Impact of annealing on the rotating frame spin-lattice relaxation time ($T_{1\rho}$) of the IgG1 protein and sucrose matrix in the P10S10 formulation studied by solid state ^{13}C NMR at 25°C. Error bars represent the uncertainty from the best fit of data to the model.

annealing of ECA/sugar formulations, no systematic differences in $\langle u^2 \rangle$ were observed for either ECA/sucrose and ECA/trehalose samples.

The local molecular motion in the protein sample was also studied with high-resolution solid-state ^{13}C NMR. Due to the specificity of the technique, it is possible to separate the motions in the protein molecule at 180 ppm due to the IgG1 carbonyl carbon from motions of sucrose at 80 ppm, Figure 7 shows the spin-lattice relaxation times ($T_{1\rho}$) in the protein and the sucrose molecules upon annealing at different conditions. Annealing at 60°C for 10 h did not cause a significant change in $T_{1\rho}$ relaxation time in either protein or sucrose molecules. Strong annealing of the protein sample at 75°C for 20 h still did not produce an obvious change in relaxation time for either protein or sucrose molecules. Thus, it seems that even though the global molecular mobility was significantly impacted by these annealing conditions, the local dynamics studied by both neutron scattering and ^{13}C NMR were not affected by annealing in the IgG1 protein/sucrose system. Since motions monitored by neutron scattering and ^{13}C NMR have different time and length scales, these different techniques may detect different parts of the local motions in the system. Given the consistent results by both techniques, we conclude that, contrary to the impact of annealing on both global mobility (i.e., TAM measured) and stability, annealing does not significantly affect local motions of the protein system, at least for the annealing conditions investigated.

However, the impact of annealing on local mobility does seem to be variable, as documented in the literature.[41,56-63] Thus, the impact of physical aging on the local mobility (beta relaxation) may depend on the nature of the sample, aging conditions, and/or detection techniques.[27] Large protein molecules are quite different from small organic molecules in that they have unique internal protein motions such as partial unfolding transitions;[50,64] thus different motions may be measured in protein systems than in synthetic polymers or small molecule organic systems, even when using the same technique.

Correlation of Stability With Protein Structure and Molecular Mobility

FTIR structure of the protein does not change significantly upon annealing for either protein formulation. However, the long-term stability clearly increases upon annealing as shown by the decrease in the aggregation rate constant. Obviously, changes in protein secondary structure are not the origin of the improved stability upon annealing, and thus we look to changes in dynamics as the mechanism to account for the stability trends.

We note that, in our system, the protein stability does not correlate with glass transition temperature. It has been reported that the degradation rate of a pharmaceutical correlates with $T-T_g$, at least for several systems,[51,54] where formulation with a higher T_g may show better stability. However, T_g of the IgG1 protein formulations is not significantly impacted by the annealing, as noticed by DSC. Also the formulation of P10S10 gives much better stability than that of P10S5 even though P10S10 has a lower T_g that P10S5. Thus, a formulation with high T_g does not necessarily mean better stability, and $T-T_g$ is not a good predictor of protein stability, at least at temperature well below T_g.[5,25,28]

Figure 8 shows the correlation of stability of P10S10 with global mobility at different annealing temperatures. For 10 h annealing (Fig. 8A), the increase in the annealing temperature caused a decrease in the aggregation rate constant and the global mobility $(1/\tau^\beta)$. Thus, the improved stability upon annealing correlates qualitatively with reduced global mobility. Also, in order to evaluate the suitability of using DSC to correlate with stability, the trend of the relaxation function (Φ) upon annealing, calculated using Eq. (2), is also given in the graph. It is noticed that the
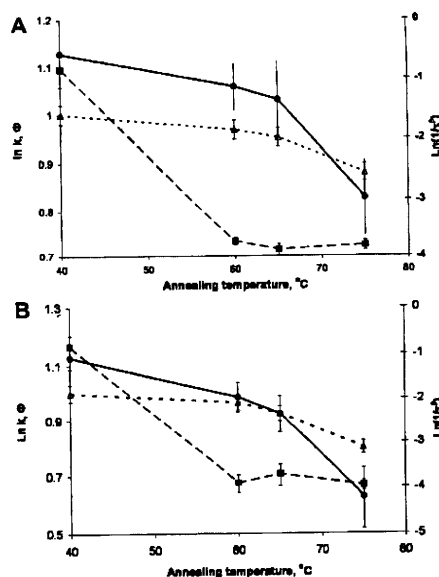

Figure 8. The relationship between physical stability ($\bullet$, ln$k$), structural relaxation time($\blacksquare$, ln($1/\tau^\beta$)), and initial relaxation function($\triangle$, Φ) for the P10S10 formulation after annealing for 10 h (A) and 20 h (B) at different temperatures. Error bars represent standard errors.

relaxation function decrease monotonically with increasing annealing temperature, which correlates with the decrease in the global mobility and aggregation rate constant. Therefore, similar to global mobility, the relaxation function obtained from a simple and fast DSC study may also be predictive of the protein stability. Further, the quantitative correlation with stability is better with Φ than with $1/\tau^\beta$. That is, the major change in $1/\tau^\beta$ occurs between the fresh sample and the sample annealed at 60°C, but for both the rate constant and Φ, the major change occurs between the samples annealed at 60 and 75°C. Figure 8B shows the same plot for the samples annealed at 20 h. Similar to 10 h annealing, the rate constant, global mobility, and relaxation function decrease with increase in the annealing temperature, but the quantitative correlation is best between stability and Φ. Figure 9 shows the correlation of aggregation rate constant with relaxation
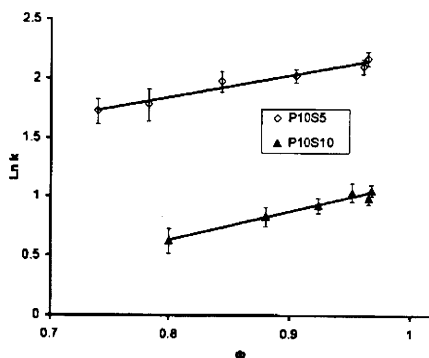
Figure 9. Correlation of protein aggregation rate with initial relaxation function (Φ) for both protein formulations. Error bar represents standard errors in the protein stability.

function for both protein formulations. Aggregation rate constants decreases with a decrease in relaxation function, showing an excellent linear correlation between $\ln(k)$ and Φ. Similar observations were made in a small molecule system (ECA/sugar system).[27] Therefore, it seems that the stability trend upon annealing may be well predicted using DSC data that is quick to obtain, uses little sample, and is quite precise relative to the structural relaxation time data obtained with isothermal calorimetry.

The better correlation of stability with Φ than with $1/\tau^\beta$ may be explained by the following factors. First, both TAM and DSC can be used to probe the enthalpy relaxation; however, these techniques may not measure exactly the same motion. It was found that the enthalpy relaxation obtained from the TAM was much higher than the enthalpy recovery obtained from DSC, which is consistent with previous observations that relaxation time constants obtained from DSC were larger than that from TAM for several systems.[65] This difference may be related to the much longer timescale for TAM experiment (several days) as compared to DSC experiment (minutes to hours), and it is possible that the TAM could measure some faster kinds of motion in addition to those motions related to enthalpy recovery (i.e., those that are mobilized only at or near the glass transition).[65] Second, it may be difficult to resolve small differences in τ^β, especially at a

high annealing temperature. In the nonlinear curve fitting procedure for the calculation of τ^β using the KWW equation,[27,48] the fitting parameters have an uncertainty associated with both τ and β. The KWW equation assumes that the relaxation time is a constant. However, aging occurs during the calorimetric experiment, and τ constantly increases with time. The impact of this in-process aging on the values of τ and β has been studied,[31,33] and it was found that this experimental procedure often gave τ values much larger than the initial value of the sample but also gave β values that were too small. However, the structural relaxation time constant, τ^β, was found to be relatively constant and representative of the constant for the initial material (i.e., before the TAM run). Therefore, τ^β is usually considered a more reliable measure of global molecular mobility. However, this parameter is still subject to significant experimental error. The errors associated with τ in annealed protein formulations were about 10–15%, as given from the nonlinear regression analysis. The results reported in Table 4 are the average τ^β of 2–3 replicates, where the uncertainty shown (generally ~10–20%) reflects standard error of the mean from the replicates. We clearly do not have the accuracy to observe small differences in τ^β, especially at high annealing temperatures. All of the above factors may contribute to the different correlations of stability with $1/\tau^\beta$ and with Φ.

In the present study, an attempt has been made to address the question "What kind of mobility is relevant for stabilization: global, local or both?" It has previously been found that stability differences between protein formulations cannot be attributed solely to differences in global mobility,[13,36,37] and local mobility may also play an important role in protein stability. Recent studies on several proteins also showed that aggregation stability correlates well with local mobility but not with either global mobility or FTIR structure over the whole range of sucrose concentration studied (mass fraction range from 0 to 0.8).[39] Thus, fast, local motions may dominate the protein stability trends at temperatures well below T_g. In the present study, we find that annealing does not significantly impact the local dynamics of the protein formulation, as measured by either NMR or neutron backscattering, and this finding is consistent with previous observations with the small molecule ECA systems studied.[27] The results obtained here suggest that it is global mobility rather than either local

mobility or FTIR structure that correlates with the improved protein stability upon annealing. Thus, with due consideration of both previous observations and the results of this study, it seems that both global and local motion are relevant for protein stabilization, even though the relative importance of each kind of mobility for stabilization could vary depending on the system and experimental conditions such as temperature, and the variable being explored. The differences chemically and physically between the samples being investigated in a stability study of the effect of annealing do differ from differences typical of the samples in a stability study. Traditional stability studies focus on variations between different formulations that generally have large differences in chemical composition, glass transition temperature, fragility, and glass strength among the formulations. However, when annealing is the variable in a stability study, the chemical composition and T_g are constant, and variation in most physical properties is minimal. Although one might expect global mobility to dominate stability trends when differences in T_g and other bulk glass properties differ greatly, and local mobility to dominate stability trends when most bulk properties differ little, we actually observed the opposite behavior. When annealing is the stability variable, it seems that global mobility is the dominant factor for long-term stability.

CONCLUSIONS

This study demonstrated, for the first time, that drying process with different thermal histories (i.e., annealing) can have a significant impact on protein stability, and thus the details of the drying process need to be defined to control product stability. Moreover, the effect of thermal history on stability may be used to further stabilize fragile protein therapeutics through the use of appropriate annealing protocols. Annealing below T_g stabilized IgG1 protein formulations by decreasing the degradation rate such that not only was the degradation rate decreased by annealing but also the annealed sample actually exhibited lower total aggregation than the control (fresh) sample after a short storage time. Thus, the concept of "stabilization by annealing" is valid for the IgG1 protein system. Annealing does not significantly impact many properties, including the SSA,

protein native structure, and local mobility; however, the enthalpy recovery and structural relaxation time constant increase upon annealing, and the improved stability upon thermal treatment is quantitatively correlated to the magnitude of relaxation function, and thus simple DSC studies may be used to guide the optimization of annealing conditions and predict stability.

REFERENCES

1. Carpenter JF, Pikal MJ, Chang BS, Randolph TW. 1997. Rational design of stable lyophilized protein formulations: Some practical advice. Pharm Res 14:969–975.
2. Costantino HR. 2004. Excipients for use in lyophilized pharmaceutical peptide, protein, and other bioproducts. In: Costantino HR, Pikal MJ, editors. Lyophilization of biopharmaceuticals. edition. Arlington, VA: AAPS Press. pp. 139–228.
3. Pikal MJ. 1990. Freeze-drying of proteins. Part II: Formulation selection. BioPharm (Duluth, MN, United States) 3:26–30.
4. Pikal MJ. 1990. Freeze-drying of proteins. Part I: Process design. BioPharm (Duluth, MN, United States) 3:18–27.
5. Hill SA, Macnaughtan W, Farhat IA, Noel TR, Parker R, Ring G, Whitcombe MJ. 2005. The effect of thermal history on the Maillard reaction in a glassy matrix. J Agric Food Chem 53:10213–10218.
6. Abdul-Fattah AM, Truong-Le V, Yee L, Nguyen L, Kalonia DS, Cicerone MT, Pikal MJ. 2007. Drying-induced variations in physico-chemical properties of amorphous pharmaceuticals and their impact on

stability (I): Stability of a monoclonal antibody. J Pharm Sci 96:1983–2008.

7. Abdul-Fattah AM, Kalonia DS, Pikal MJ. 2007. The challenge of drying method selection for protein pharmaceuticals: Product quality implications. J Pharm Sci 96:1886–1916.

8. Sartor G, Mayer E, Johari G. 1994. Thermal history and enthalpy relaxation of an interpenetrating network polymer with exceptionally broad relaxation time distribution. J Polym Sci B Polym Phys 32: 683–689.

9. Abdul-Fattah Ahmad M, Truong-Le V, Yee L, Pan E, Ao Y, Kalonia Devendra S, Pikal Michael J. 2007. Drying-induced variations in physico-chemical properties of amorphous pharmaceuticals and their impact on stability. II: Stability of a vaccine. Pharm Res 24:715–727.

10. Franks F, Hatley RHM, Mathias SF. 1991. Materials science and the production of shelf-stable biologicals. BioPharm 4:38–42.

11. Maa Y-F, Prestrelski S. 2000. Biopharmaceutical powders: Particle formation and formulation considerations. Curr Pharm Biotechnol 1:283–302.

12. Pikal MJ. 2004. Mechanisms of protein stabilization during freeze-drying and storage: The relative importance of thermodynamic stabilization and glassy state relaxation dynamics. Drugs Pharm Sci 137:63–107.

13. Yoshioka S, Aso Y. 2007. Correlations between molecular mobility and chemical stability during storage of amorphous pharmaceuticals. J Pharm Sci 96:960–981.

14. Wang W. 2000. Lyophilization and development of solid protein pharmaceuticals. Int J Pharm 203: 1–60.

15. Pikal MJ. 2002. Chemistry in solid amorphous matrices: Implication for biostabilization. In: Levine H, editor. Amorphous food and pharmaceutical systems. edition. Cambridge, UK: The Royal Society of Chemistry. pp. 257–277.

16. Guo Y, Byrn SR, Zografi G. 2000. Physical characteristics and chemical degradation of amorphous quinapril hydrochloride. J Pharm Sci 89:128–143.

17. Duddu SP, Zhang G, Dal Monte PR. 1997. The relationship between protein aggregation and molecular mobility below the glass transition temperature of lyophilized formulations containing a monoclonal antibody. Pharm Res 14:596–600.

18. Shamblin SL, Hancock BC, Pikal MJ. 2006. Coupling between chemical reactivity and structural relaxation in pharmaceutical glasses. Pharm Res 23:2254–2268.

19. Pikal MJ, Rigsbee D, Roy ML, Galreath D, Kovach KJ, Wang B, Carpenter JF, Cicerone MT. 2008. Solid state chemistry of proteins: II. The correlation of storage stability of freeze-dried human growth

hormone (hGH) with structure and dynamics in the glassy solid. J Pharm Sci 97:5106–5121.

20. Yoshioka S, Aso Y. 2005. A quantitative assessment of the significance of molecular mobility as a determinant for the stability of lyophilized insulin formulations. Pharm Res 22:1358–1364.

21. Yoshioka S, Aso Y, Miyazaki T. 2006. Negligible contribution of molecular mobility to the degradation rate of insulin lyophilized with poly(vinylpyrrolidone). J Pharm Sci 95:939–943.

22. Struik LCE. 1978. Physical aging in amorphous polymers and other materials. edition. New York, NY: Elsevier. p. 230.

23. Hodge IM. 1994. Enthalpy relaxation and recovery in amorphous materials. J Non-Crystal Solids 169: 211–266.

24. Pikal MJ. 1996. Thermometric seminars on calorimetry in materials sciences, Stockholm, Sweden.

25. Abdul-Fattah AM, Dellerman KM, Bogner RH, Pikal MJ. 2007. The effect of annealing on the stability of amorphous solids: Chemical stability of freeze-dried moxalactam. J Pharm Sci 96:1237–1250.

26. Luthra SA, Hodge IM, Utz M, Pikal MJ. 2008. Correlation of annealing with chemical stability in lyophilized pharmaceutical glasses. J Pharm Sci 97:5240–5251.

27. Wang B, Pikal MJ. The impact of thermal treatment on the stability of freeze dried amorphous pharmaceuticals: I. Dimer formation in sodium ethacrynate. J Pharm Sci: In press.

28. Carpenter JF, Prestrelski SJ, Anchordoquy TJ, Arakawa T. 1994. Interactions of stabilizers with proteins during freezing and drying. ACS Symposium Series (Formulation and Delivery of Proteins and Peptides), Vol. 567, pp. 134–147.

29. Chang L, Shepherd D, Sun J, Ouellette D, Grant KL, Tang X, Pikal MJ. 2005. Mechanism of protein stabilization by sugars during freeze-drying and storage: Native structure preservation, specific interaction, and/or immobilization in a glassy matrix? J Pharm Sci 94:1427–1444.

30. Shamblin SL, Zografi G. 1998. Enthalpy relaxation in binary amorphous mixtures containing sucrose. Pharm Res 15:1828–1834.

31. Liu J, Rigsbee DR, Stotz C, Pikal MJ. 2002. Dynamics of pharmaceutical amorphous solids: The study of enthalpy relaxation by isothermal microcalorimetry. J Pharm Sci 91:1853–1862.

32. Pikal MJ, Chang L, Tang X. 2004. Evaluation of glassy-state dynamics from the width of the glass transition: Results from theoretical simulation of differential scanning calorimetry and comparisons with experiment. J Pharm Sci 93:981–994.

33. Kawakami K, Pikal MJ. 2005. Calorimetric investigation of the structural relaxation of amorphous materials: Evaluating validity of the methodologies. J Pharm Sci 94:948–965.